Highly Productive Ice Algal Mats in Arctic Melt Ponds: Primary Production and Carbon Turnover

Kasper Hancke[1]*, Svein Kristiansen[2] and Lars Chresten Lund-Hansen[3]

[1] Section for Marine Biology, Norwegian Institute for Water Research, Oslo, Norway, [2] Department of Arctic and Marine Biology, UiT - The Arctic University of Norway, Tromsø, Norway, [3] Arctic Research Center & Aquatic Biology, Department of Biology, Aarhus University, Aarhus, Denmark

Arctic summer sea ice extent is decreasing and thinning, forming melt ponds that cover more than 50% of the sea ice area during the peak of the melting season. Despite of this, ice algal communities in melt ponds are understudied and so are their contribution to the Arctic Ocean primary production and carbon turnover. While melt ponds have been considered as low productive, recent studies suggest that accumulated ice algal potentially facilitate high and yet overlooked rates of carbon turnover. Here we report on ice algal communities forming dense mats not previously described, collected from melt ponds in the northern Barents Sea in July. We document on distinct layered and brown colored mats with high carbon assimilation and net primary production rates compared to ice algal communities and aggregates, in fact comparable to benthic microalgae at temperate tidal flats. Rates of gross and net primary production, as well as community respiration rates were obtained from oxygen micro profiling, and carbon assimilation calculations were supported by ^{14}C incubations, pigment analysis and light microscopy examinations. The melt pond algal mats consisted of distinct colored layers and differed from aggregates with a consisted layered structure. We accordingly propose the term melt pond algal mats, and further speculate that these dense ice algal mats may provide an important yet overlooked source of organic carbon in the Arctic food-web. A foodweb component likely very sensitive to climate driven changes in the Arctic Ocean and pan-Arctic seas.

Keywords: ice algae, melt ponds, oxygen production and consumption, photosynthesis, carbon turnover, Arctic Ocean

INTRODUCTION

Ice algae residing at the bottom of the sea ice and in brine channels contribute about 10% of the total marine-produced organic carbon in the Arctic Ocean (Arrigo, 2017). In the permanently ice covered central Arctic Ocean, their relative contribution is likely much higher and have been reported to 57% of the entire primary production (water column and sea ice, Gosselin et al., 1997). The total primary production in the central Arctic Ocean was in 1997 estimated to 15 g C m^{-2} year^{-1}, a value upgraded

more than 10 times relative to previously reports (English, 1961; Gosselin et al., 1997). More recently, the central Arctic primary production and net carbon fixation rates have been suggested to range from 1 to 25 g C m^{-2} year^{-1} comprising phytoplankton and sympagic ice algae productivity in and underneath the sea ice (Boetius et al., 2013). The contribution of ice algae is, however, not well constrained ranging from 0 to 80% (Boetius et al., 2013) and showing large variability (Campbell et al., 2022).

Timing of the ice algae production is crucial to the food web as being a key organic carbon source for higher trophic levels in permanently ice-covered regions and during ice-covered periods in early spring, when the pelagic productivity is low (Leu et al., 2015). For instance, it has been shown that 70 to 100% of polar bears' (*Ursus maritimus*) carbon intake relied on sympagic production (Brown et al., 2018), stressing the importance of ice algae in sustaining the Arctic ecosystem. This production is generally located at or near the bottom of the sea ice (Arrigo, 2017), where ice algae have adapted to extreme low light conditions (Hancke et al., 2018). Also, ice algae have been demonstrated an important carbon source for the benthic food web in the deep-sea (Tamelander et al., 2009; Boetius et al., 2013; Lalande et al., 2019). In recent years, there has been an enhanced research focus on ice algae communities and algae aggregates (Katlein et al., 2015) which float below the sea ice (Assmy et al., 2013), in leads (Fernández-Méndez et al., 2014), and in melt ponds (Lee et al., 2011). The aggregates consist generally of agglutinated diatoms of the common Arctic diatom *Melosira* sp. and show comparatively high carbon production rates (Assmy et al., 2013).

Arctic marine ecosystems are experiencing dramatic environmental changes (Babin, 2020), including warming at rates two to four times faster than the global average (Meredith et al., 2019). This leads to thinning and loss of sea ice in the Arctic Ocean (Cavalieri and Parkinson, 2012; Wunderling et al., 2020), with pronounced consequences for ice algal productivity, carbon turnover, and the Arctic food web (Leu et al., 2015). Warming is also accelerating the formation of melt ponds, that have been estimated to cover more than 50-60% of the sea ice area during peak of the melting season (Lee et al., 2020). Despite of this, ice algae communities in melt ponds are understudied and so is their contribution to Arctic primary production and carbon turnover.

Here we report on ice algae mat-like communities not previously described in the Arctic, with the objective to quantify the rate of carbon assimilation and net primary production. The mats were collected from melt ponds in the northern Barents Sea in July, and observations are compared with published data on microalgal productivity. We speculate that these melt pond algal mats constitute an unexplored carbon source that could be important for the biogeochemical cycling in the Arctic Ocean.

MATERIALS AND METHODS

Study Area, Sampling, and Experimental Setup

Clearly layered mats of dense microalgae communities, hereafter referred to as melt pond algal mats, were collected from sea ice melt ponds at N 82° 24.9 and E 30° 26.2 during a cruise in the Barents Sea in July 2004 (**Figures 1A, B**) as part of a large Arctic ecosystem research project (CABANERA, Wassman et al., 2008). The mats were initially between 3 and 10 cm wide but broke up in smaller pieces (1-3 cm across) during sampling even at gentle handling. The mats were 3.5 to 4 mm thick with distinct and coherent layers stacked in visually recognized brown colored layers (**Figure 1C**). The sea ice melt ponds from where the mats were sampled were open at the bottom, i.e. there was a free flow of water between the melt pond and the ocean below. The melt pond was located near the center of the ice floe characterized as pack ice due to the occurrence of ridges and hummocks, and ice thickness varied from 1 to 1.5 m. During the available time on the ice we collected 10 to 15 algal mats from five melt ponds on the same ice flow, that were subsequently brought back to the onboard lab. The mats was gently sampled in cleaned polyethylene containers with *in situ* water from the melt pond, having a salinity of 34.0 and a temperature of ~0°C. The sampling location is further described in Wassmann et al. (2008).

Photosynthesis and respiration rates were measured after installing intact pieces of the algal mat in a microcosm that mimicked the *in situ* conditions within half an hour after sampling (**Figure 1D**). Three mats were sequentially installed and measured in the microcosm. The microcosmos was established inside a cold room (2.0°C) on board the research vessel and the microcosms temperature was secured at 0°C using an additional cooling device, in a setup equivalent to what was used by Hancke and Glud (2004). The algal mat was carefully pinned to a white styrofoam plate submerged in the microcosms that mimicked the light reflection properties of sea ice and kept the mat in a fixed position during measurements. Flushing gently with an air pump ensured both a stable diffusive boundary layer (DBL) of 300 to 500 μm over the mat and keeping the oxygen (O_2) concentration of the water at atmospheric saturation level. The mat surface was exposed to a photosynthetically active radiation (PAR) of 400 μmol photons m^{-2} s^{-1} during photosynthesis measurements by a halogen lamp with an optical fiber (Schott KL 1500). The irradiance was chosen to represent average light conditions in the melt ponds based on measured ambient light, which diel variations between 200 and 1200 μmol photons m^{-2} s^{-1} and an average of ~400 μmol photons m^{-2} s^{-1} at sampling time in July. Incident PAR was measured with a LiCor cosine-corrected quantum sensor and logger (LiCor LI-190SA, LiCor LI-1000, LiCor, US.).

Oxygen Production and Consumption

Oxygen micro profiles were measured using electrochemical O_2 microsensors with a guard cathode (Revsbech, 1989) provided by RN Glud's laboratory (University of Southern Denmark, DK). Gross and net photosynthesis, and dark community respiration were estimated from profiles measured using electrodes with tip diameters <15 μm, stirring sensitivity <1% and a 90% response time <0.5 s. Electrodes were calibrated by a 2-point calibration performed in both anoxic and air-saturated samples at ambient temperature. See Glud et al. (2000) and Hancke and Glud (2004) for additional details of the microsensor setup.
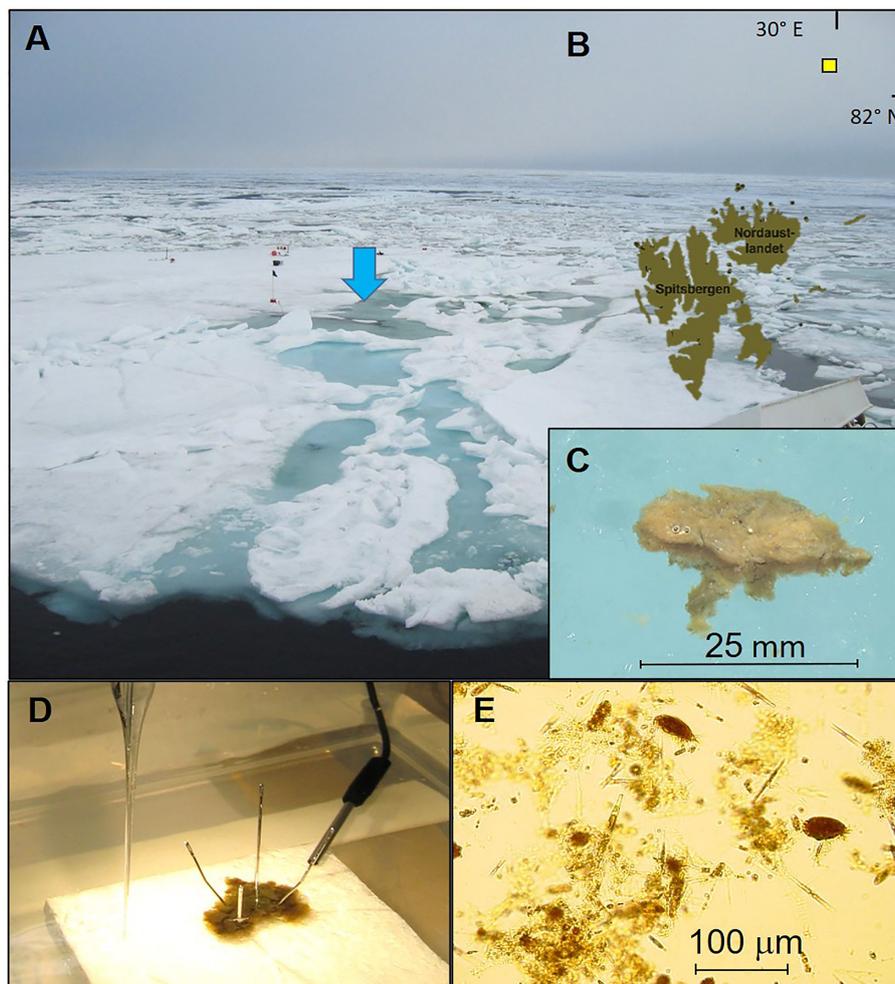
FIGURE 1 | Ice floe at the sampling site where the ice algal mats were collected (marked with blue arrow) with open and closed melt ponds **(A)**, and the sampling position at N 82° 24.9 marked with a yellow square in **(B)** to the NE of Svalbard. Close up of the sampled algal material that was recognized as brown-colored coherent mats with a clearly layered structure **(C)**. The mats were initially between 3 and 10 cm wide but broke up in smaller pieces (1-3 cm across) during sampling and transport to the lab onboard the research vessel. An experimental setup with controlled temperature and light conditions were established to measure gross and net O_2 production in the mats **(D)**, that consisted of a complex community of microalgae and diverse grazers including ciliates **(E)**. Photos by the authors (K. Hancke).

Gross photosynthesis was measured by the light-dark shift method (Revsbech and Jorgensen, 1983; Glud et al., 1992), by estimating the gross O_2 production from the initial concentration decline after a sudden eclipse of light (triplicates, with 3 min intervals). Total gross photosynthesis of the mat was calculated from integrating stepwise measurements down through the mat. Gross O_2 production was eventually converted to gross C fixation by multiplying with the molecular weight for C (12), the photosynthetic coefficient (1.4), and assuming 24h of daylight.

Rates of community net photosynthesis and dark respiration were calculated from the derived slope coefficient of the oxygen concentration profiles across the diffusive boundary layer and the top layer of the algal mat during light and dark, respectively (Jørgensen and Revsbech, 1985, **Figure 2**). Net photosynthesis equaled the flux of O_2 out of the illuminated mat, while respiration equaled influx during darkness. The community net photosynthesis and respiration rates were calculated from the sum of the upward and downward flux rates, derived from the linear concentration gradient during steady-state conditions, using Fick's first law of diffusion (Jørgensen and Revsbech, 1985). Rates were corrected for the molecular diffusion coefficient according to Broecker and Peng (1974) and for temperature and salinity (Li and Gregory, 1974). Oxygen profiles varied little laterally across several investigated mats pieces and all derived rates were obtained from triplicated profiling. Flux rate calculations and the underlying principles are further described in Jørgensen and Revsbech (1985); Kühl et al. (1996); Glud et al. (2002) and Hancke and Glud (2004).
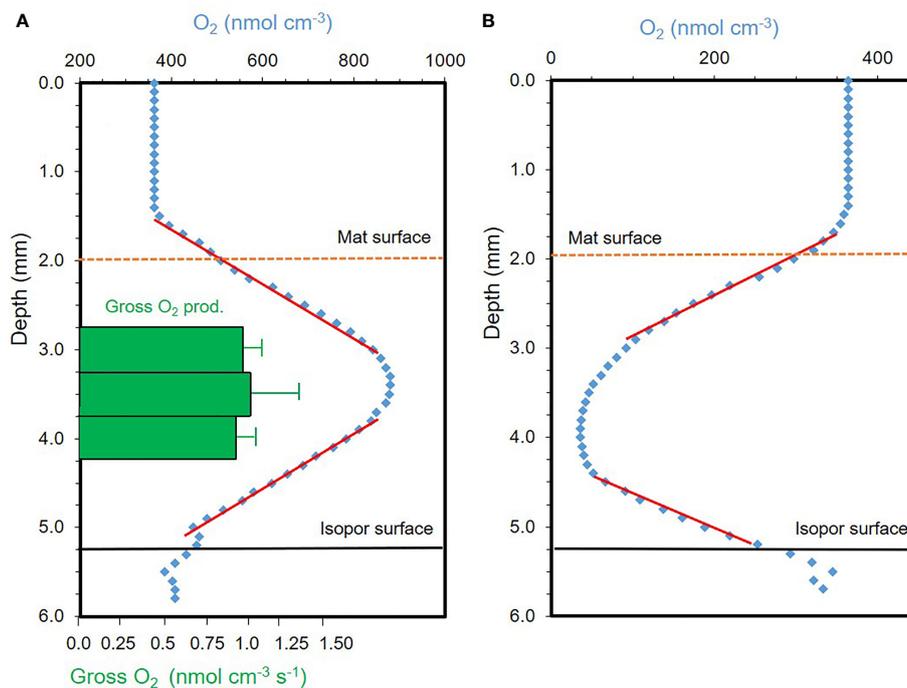
FIGURE 2 | Steady state oxygen concentration profiles through melt pond algal mats (blue dots) collected from Arctic sea ice melt ponds in **(A)** light (400 µmol photons m^{-2} s^{-1}), and **(B)** darkness, respectively. Net O_2 production in the light, and dark O_2 consumption was calculated from the derived slope coefficients (red lines), respectively. Green bars in **(A)** represent the depth-resolved gross oxygen production derived independently from the net production, by the light-dark method (see M&M). The oxygen concentration profiles demonstrated a pronounced oxygen consumption in the dark that was surpassed by the oxygen production in light, driven by the exceeding gross production.

^{14}C Assimilation

Gross ^{14}C fixation was measured using the benchmark ^{14}C method (Stemann-Nielsen, 1952). Subsamples of the three mats were incubated for four hours in pre-filtered (GF/F microfiber filters, Whatman, US) *in situ* water in light (400 µmol photons m^{-2} s^{-1}) and in dark polycarbonate bottles positioned in the microcosms, with a final concentration of 0.0125 µCi mL^{-1}. Samples were subsequently filtered and immediately frozen onboard. Within 2 months filters were thawed, fumed with HCl acid for 8 hours, and 10 mL of Ultima GoldTM XP (Packard) were added before counting on a liquid scintillation analyzer with quench correction (PerkinElmer Tri-Carb 2900TR). The dark bottle values were subtracted from the light bottle values. The method is described in detail in Hodal and Kristiansen (2008), and the gross carbon fixation rate was corrected for total inorganic carbon based on Kivimae (2007).

Chlorophyll *a*, Carbon, and Nitrogen

Subsamples were taken by cutting cross sections from top to bottom of the mat and thus collecting pieces with known surface area and ensuring that the complete mat-structure was represented, and subsequently filtered on GF/F filters. Chlorophyll *a* (Chl *a*) was calculated from three subsamples extracted in MeOH (6h, 5°C, darkness) and measured

absorbance at 665 nm, subtracting the absorbance at 750 nm, and using an extinction coefficient of 74.5 L g^{-1} cm^{-1} (Mackinney, 1941). The procedure is further described in Hancke et al. (2008). Likewise was particulate organic carbon (POC) analyzed following standard procedures after treatment of the samples with hydrochloric acid to remove the inorganic fraction using a Carlo Erba Elemental Analyzer (Model Na; Carlo Erba, Italy). Particulate organic nitrogen (PON) was analyzed according to Grasshoff et al. (1999) using a Scalar autoanalyzer (Scan Plus System, Netherlands). Mat wet and dry weights (dried in oven for >12h at 80°C) were determined to provide uniform measures and convert from areal to carbon units for gross photosynthesis measures.

Photosynthetic Pigments and Light Microscope Analysis

Pigment samples were stored at -80°C until analyzed using a Hewlett-Packard HPLC 1100 Series system, equipped with a quaternary pump system and diode array detector. Mat subsamples were extracted in MeOH overnight at –20°C, and pigments were separated in Waters Symmetry C8 column (150 × 4.6 mm, 3.5 µm particle size) according to Zapata et al. (2000) and modified by Rodriguez et al. (2006). The extract was re-filtered (Millipore 0.2 µm) to remove debris. Chlorophylls and carotenoids were quantified according to their absorbance

(350-750 nm). Identification of pigments and specific extinction coefficients for quantification followed Jeffrey et al. (1999). Light microscope analysis was used to identify dominant algal groups and species along with characterizing the community of grazers in the mat, before and after addition of Lugol (Tomas, 1997).

RESULTS

Dark Respiration, Net and Gross Photosynthesis in the Algal Mat

Steady state O_2 concentration profiles through the mat showed distinct gradients from the water above to the center of the algal mat, which was almost mirrored from the mat center and downward to below the mat. In the light (**Figure 2A**), O_2 concentration increased with depth until the center of the mat which indicated a photosynthetically active algal community with a high O_2 production, that by far exceeded the respiratory O_2 demand. At 400 μmol photons m^{-2} s^{-1}, steady state O_2 profiles showed concentrations of >800 nmol O_2 cm^{-3} (equivalent to μmol O_2 L^{-1}) in the mat center, a more than doubled O_2 concentration relative to the ambient level. In the dark (**Figure 2B**), the O_2 concentration decreased from atmospheric saturation in the above water (363 nmol O_2 cm^{-3}) to <40 nmol O_2 cm^{-3} at the center of the mat, about 1.5 to 2 mm into the mat. The steep decrease in the O_2 concentration reflected a pronounced O_2 consumption in the mat during darkness.

The mat net community production of O_2 in light was 0.077 ± 0.008 nmol O_2 cm^{-2} s^{-1} (n=3), equivalent to 798 ± 83.0 mg C m^{-2} d^{-1} (assuming a molar ratio for O_2:C of 1:1 and a 24h day period equivalent to midnight sun, **Figure 3**). Algal mat community O_2 consumption in the dark was 0.067 ± 0.0054 nmol O_2 cm^{-2} s^{-1} (n=3), equivalent to 695 ± 55.6 mg C m^{-2} d^{-1}. The photosynthetic gross O_2 production was 0.101 ± 0.016 nmol O_2 cm^{-2} s^{-1} (n=3), equal to 1467 ± 246 mg C m^{-2} d^{-1} (24h daylight, **Figure 3**). This measure was derived from the light-dark shift method and integrated over the center 1 mm thick photosynthetic zone in the mat (**Figure 2A**). The measure is independent of the net photosynthetic rate (**Figure 3**). Gross photosynthesis was in addition measured as the rate of gross ^{14}C fixation in intact subsamples of the mat of a known area (~1.5 cm^2) and weight. Gross ^{14}C fixation equaled 2627 ± 305 mg C m^{-2} d^{-1} (n= 3). The ^{14}C method showed gross carbon fixation rates more than twice as high as the measured gross O_2 production, which demonstrates a highly productive photosynthetic community. The method is, however, sensitive to the precision of the determined area, in contrast to the microsensor results.

Chl a, C, and Photosynthetic Pigments

The Chl *a* concentration in the mat was 46.9 ± 6.7 mg Chl *a* m^{-2}, the POC content 3412 ± 686 mg C m^{-2}, and the PON content 406 ± 92.8 mg N m^{-2}. This corresponded to ratios of C:Chl *a* = 75.1 ± 25.7, and of C:N = 9.8 ± 0.5 (**Table 1**). HPLC analyses showed a fucoxanthin content of 60% and a diadinoxanthin content (typical sunscreen pigment) of 30% of the Chl *a*

concentration. The ratio of total photoprotective versus photosynthetic pigments were 0.18 ± 0.004 (n=3).

Light Microscope Analysis

Light microscope analyses showed a dominance of the following algal genera *Nitzschia* spp., *Navicula* spp., *Amphiprora* spp., *Entomoneis* spp., and *Pleurosigma* spp. Also, a high representation of grazers including ciliate species were observed in the mats (**Figure 1E**), corresponding to previous observations of melt pond algal mats (Sørensen et al., 2017). Species composition of the grazer community was not further investigated.

DISCUSSION

Melt Pond Ice Algal Mat Structure and Formation

The sampled ice algal mats were evidently different in physical structure and form than what has been reported previously of ice algal communities and accumulations beneath sea ice, including *Melosira* aggregates (Boetius et al., 2013) and floating aggregates (Fernández-Méndez et al., 2014). In their physical structure, they also differed from free-floating spherical algal accumulations observed in leads and below sea ice (Assmy et al., 2013). The species composition were, on the other hand, similar to previously observed floating algae aggregates and typical ice algae communities (Hegseth, 1992; Assmy et al., 2013).This indicate, that the melt pond algal mats may have a common point of origin with the spherical algal aggregates reported by Assmy et al. (2013). The observed melt pond algal mats were elongated, 3-5 mm thick with alternating light to dark brown layers (**Figure 1C**), with clear vertical layers in resemblance to other microbial and benthic mats (Franks and Stolz, 2009; Glud et al., 2009), which occur in a variety of environments as tidal flats (Barranguet et al., 1998), sublittoral soft-bottom sediments in the photic zone (Glud et al., 2002; Hancke and Glud, 2004; Woelfel et al., 2010), and in polar lakes and rivers (Quesada et al., 2008).

We speculate that the reported melt pond mats have formed at the bottom of melt ponds as a result of inflow of water and algae into open melt ponds (Fernández-Méndez et al., 2014) where the change from low light below the sea ice (<20 μmol photons m^{-2} s^{-1}, Lund-Hansen et al., 2015) to high light in the pond (200 to 1200 μmol photons m^{-2} s^{-1}) sparked the development of these dense microbial mat communities. This pair with the observations of a microalgal community that appear high-light acclimated, from the presence of the photoprotective pigment diadinoxanthin and the ratio of photoprotective versus photosynthetic pigments (Joy-Warren et al., 2019; Lund-Hansen et al., 2020). While Lee et al. (2011) reports about a new ice algal habitat formed by holes in the progressing thinning Arctic sea ice, they describe the formation and aggregation of ice algae to form long strands extending into the water below. This contrasts with our observations of distinct algal mats that have physical characteristics as benthic microphyte mats. Moreover, Lee et al. reports a dominance of
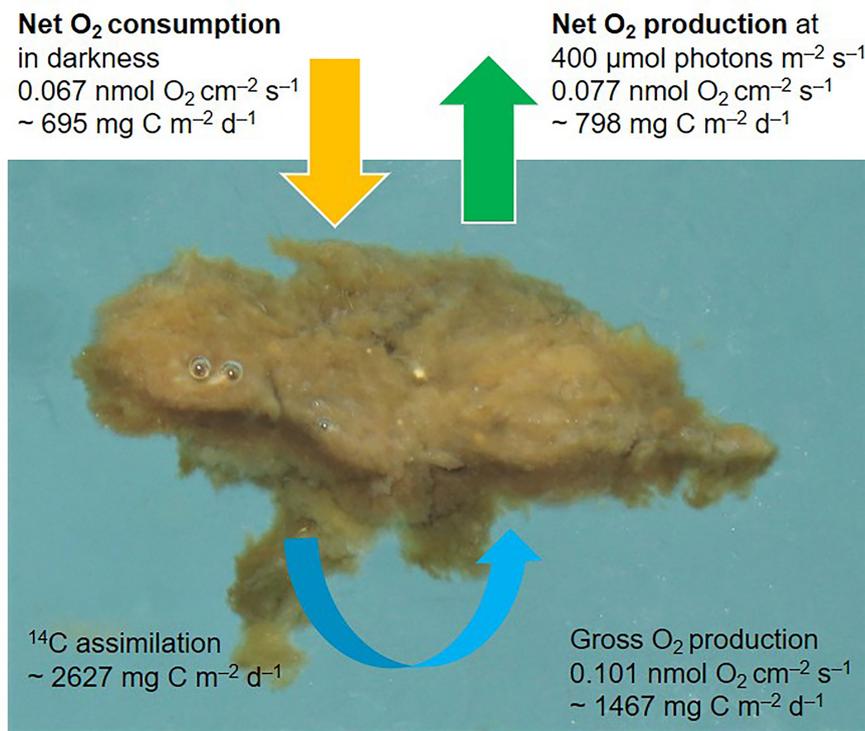
FIGURE 3 | Rates of dark oxygen respiration (yellow arrow), net community production (green arrow), and gross oxygen production (blue arrow) in a melt pond algal mat, derived from oxygen concentration profiles and ^{14}C-assimilations. Units per surface area of the mat in nmol O_2 cm^{-2} s^{-1} and the equivalent in mg C m^{-2} d^{-1}, assuming a O_2:C ratio of 1.0 for net rates and 1.4 for gross production, under 24h sunlight (midnight sun). Note the small bubbles of oxygen on the mat surface to the left, which originate from O_2 supersaturation and indicate a high net community O_2 production within the mat. Photo by K. Hancke.

Melosira arctica (>95%) with *Nitzschia* and *Navicula* species contributing the remaining. To our knowledge there is no previous reports on ice algal mats as we describe them here.

We do not know, over how much time the melt pond algal mats developed. The melt ponds were open upon sampling (free connection to the under-ice water), which we speculate is a precursor for the mat formation, and enables a continuous supply of nutrient rich water from below, as closed melt ponds typically hold low nutrient concentrations (Lee et al., 2011; Sørensen et al., 2017). The open melt ponds are regarded as the last development stage of the sea ice before freezing over in early autumn (Lee et al., 2011). This leaves a proposed window

TABLE 1 | Primary production rates (gross or net), concentrations of Chl a, particulate organic carbon (POC) and nitrogen (PON), and ratios of C:N and C:Chl a in the present melt pond algae mat and previous reports for sea ice algae, ice algae aggregates, benthic algae, and microbial mats.

Type/Unit	PP mg C m^{-2} h^{-1}	Chl a mg m^{-2}	POC mg m^{-2}	PON mg m^{-2}	C:N	C:Chl a	Ref,
Melt pond algal mats	33[N,O] 109[C,G]	47 ± 6.7	3412 ± 686	406 ± 93	9.8 ± 0.5	75 ± 26	This study
Ice algae					8.5 ± 1.7	21.4 ± 12.8	(Hegseth, 1992)
Ice algae	0.008-19.3[O,C,H]	75			10.6 ± 1.7	66.8 ± 23.4	(Arrigo, 2017)
Ice algae		<0.5 - 15					(Gosselin et al., 1997)
Aggregates		52-200					(Gosselin et al., 1997)
Aggregates	0.0001-0.001[C,H,N]	0.0017-0.0063	0.19-1.33	0.03-0.17	7.9-9.1	21.2-112	(Assmy et al., 2013)
Aggregates	0.02-0.25[O,H]	2.94					(Glud et al., 2014)
Aggregates	0.02-0.4[C,N]	0.1-3.7	11-793	1-72	11-35	500-66700	(Fernández-Méndez et al., 2014)
Melosira filaments	0.54-1,67[C,N,H]	14-44	3020-9094	108-324	10-40	850-4600	(Fernández-Méndez et al., 2014)
Benthic microalgae (Svalbard)	1-23[O]	13-317					(Woelfel et al., 2010)
Benthic microalgae mats (Svalbard)	2.8-14.6[N,O]	2.7 ± 0.7					(Hancke and Glud, 2004)
Benthic microalgae mats (Denmark)	25.7-55.2[N,O]	22.9 ± 6.5					(Hancke and Glud, 2004)
Benthic microalgae mats (Netherlands)	10-100[C,G]	15-32					(Barranguet et al., 1998)

C:N (atm:atm), C:Chl a (w:w). Letters abbreviate the following, N, Net primary production; C, ^{14}C method; G, Gross primary production; O, O_2 method.; H, converted into h^{-1} for comparative reasons.

for the development of these melt pond algal mats of about one month around July-August before freezing and snowfall in late August/early September.

The Chl *a* concentration in the melt pond algal mats (46.9 ± 6.7 mg m^{-2}) was higher than most reports of ice algal communities in the Arctic when scaled up to a common areal unit, including aggregated ice algae (Assmy et al., 2013; Fernández-Méndez et al., 2014; Glud et al., 2014), and under-ice algal communities (Gosselin et al., 1997, **Table 1**). Even when compared to microphytobenthic mats in arctic and temperate environments with dense and photosynthetic active algal communities (Barranguet et al., 1998; Glud et al., 2002; Hancke and Glud, 2004; Woelfel et al., 2010). Nevertheless, higher concentrations of Chl *a* have been reported for ice algae in both Arctic and Antarctica than we observed here (Vincent et al., 1993; Arrigo, 2017). See Leu et al. (2015) for a pan-Arctic review of ice algal abundances.

Primary Production and Carbon Turnover

In general, melt ponds of the Arctic Ocean are considered as low productive however empirical evidence is sparse and scattered (Lee et al., 2015; Sørensen et al., 2017). The rapidly warming Arctic favors first year ice over multiyear ice, which again is leading to an increase in melt pond formation and coverage (Polashenski et al., 2012). Warming has also been suggested to decrease ice algal primary production throughout the Arctic due to a shorter growth season (Leu et al., 2015), at the same time the contribution to primary production and carbon turnover by melt pond algal might increase due to the increase in areal coverage.

We here report on highly productive melt pond algal mat with a gross carbon production (2627 mg C m^{-2} d^{-1}) that largely exceeded the dark consumption (695 mg C m^{-2} d^{-1}), and thus resulted in a high net community production. The net community production was approximate two times higher when calculated from gross ^{14}C fixation (minus the dark C consumption, as conventionally done) than when estimated independently from the O$_2$ steady state profiles (**Figure 3**). This was however anticipated, as ^{14}C-samples were incubated in suspension which decreased the degree of self-shading between algae and thus can lead to overestimation of the gross carbon fixation (Stemann-Nielsen, 1952). Contrasting, the O$_2$ electrode method likely underestimates true gross O$_2$ production as it only includes photosynthetic production from the core of the mat (green bars in **Figure 2**) excluding peripheral algae photosynthesis (Glud et al., 1999). Nevertheless, the ice algal mat community demonstrated the highest net production rate of Arctic ice algal communities reported (**Table 1**). In fact, the present melt pond algal mat rates were approximately 3 times higher compared to measured rates from benthic algal microbial mats on temperate tidal flats.

Largely, ice algae are reported to sustain a low primary production in the Arctic, but large variations have been observed between regions, ice types, and habitats (Hegseth, 1992; Gosselin et al., 1997; Assmy et al., 2013; Glud et al., 2014; Arrigo, 2017; Lund-Hansen et al., 2018; Campbell et al., 2022). Low productivity of ice algal and aggregate communities

is often associated with snow and ice cover and consequently often is light-limited (Woelfel et al., 2010; Leu et al., 2015; Hancke et al., 2018; Lund-Hansen et al., 2020b; Lund-Hansen et al., 2020a). In contrast, temperate benthic algal mats and the here described melt pond mats are both exposed to high light. In this case, it is reasonable to assume, that high primary production rates were supported by high light conditions prevailing at the bottom of melt ponds in combination with access to nutrient rich water from below the ice. This compares well with high rates of biological activity reported for floating ice-algal aggregates when scaled to the individual aggregate size published by Assmy et al. (2013), leading the authors to suggest that algae aggregates may provide a concentrated food source for ice-associated fauna during the oligotrophic Arctic summer months.

The fraction of melt ponds covering the sea ice in the Arctic Ocean in July is reported to be as high as 50 to 60% (Lee et al., 2020) but carbon fixation often low, estimated to <1% of the carbon production (Lee et al., 2012), with rates around 1.0 mg C m^{-2} d^{-1} (Sørensen et al., 2017). The net rate of 798 mg C m^{-2} d^{-1} measured in the algal mat demonstrates that melt pond algal mats may represent a significant carbon source for grazing and benthic organisms, as also suggested by Boetius et al. (2013), but how prevalent these mats are is still unanswered. Considering the research focus on ice algae, melt ponds and aggregates during the last two decades it is remarkable that mats similar to what we report here, have not been published even after we made our observations in 2004, which might imply that the mats have a low prevalence. Thus, their overall contribution to the Arctic Ocean carbon turnover is uncertain. However, our results suggest that melt pond algal mats might contribute to the Arctic Ocean carbon and energy flow at least on local and possible on regional scales. In addition, one might speculate that summer 'blooms' of algal mats in melt ponds could add an unpreceded supply of carbon to the Arctic food web late in the season. Additional measures of primary productivity and carbon turnover in melt pond algal mats alongside with quantification of their abundance and distribution are needed. Not least to understand the impact of increased warming on Arctic carbon pathways. Possibly, modern remote sensing techniques such as flying drones with high resolution imaging sensors (typical >1000 times better resolution than satellites) might provide tools to disclose the abundance and distribution of ice algal mats in melt ponds in the future.

DATA AVAILABILITY STATEMENT

The original contributions presented in the study are included in the article/supplementary material. Further inquiries can be directed to the corresponding author.

ETHICS STATEMENT

Sampling and handling of samples followed general and acknowledged practices.

AUTHOR CONTRIBUTIONS

FUNDING

ACKNOWLEDGMENTS

REFERENCES

Arrigo, K. R. (2017). "Sea Ice as a Habitat for Primary Producers,". Ed. D. N. Thomas (Sea Ice. Oxford: Wiley Blackwell. 3rd), pp. 352–369.

Assmy, P., Ehn, J., Fernández-Méndez, M., Hop, H., Katlein, C., Sundfjord, A., et al. (2013). Floating Ice-Algal Aggregates Below Melting Arctic Sea Ice. *PloS One* 8, e76599. doi: 10.1371/journal.pone.0076599

Babin, M. (2020). Climate Change Tweaks Arctic Marine Ecosystems. *Science* 369, 137–138. doi: 10.1126/science.abd1231

Barranguet, C., Kromkamp, J., and Peene, J. (1998). Factors Controlling Primary Production and Photosynthetic Characteristics of Intertidal Microphytobenthos. *Mar. Ecol. Prog. Ser.* 173, 117–126. doi: 10.3354/meps173117

Boetius, A., Albrecht, S., Bakker, S., Beinhold, C., Felden, J., Fernández-Méndez, M., et al. (2013). Export of Algal Biomass From the Melting Arctic Sea Ice. *Science* 339, 1430–1432. doi: 10.1126/science.1231346

Broecker, W. S., and Peng, T.-H. (1974). Gas Exchange Rates Between Air and Sea. *Tellus* 34, 21–35. doi: 10.1111/j.2153-3490.1974.tb01948.x

Brown, T. A., Galicia, M. P., Thiemann, G. W., Belt, S. T., Yurkowski, D. J., and Dyck, M. G. (2018). High Contributions of Sea Ice Derived Carbon in Polar Bear (Ursus Maritimus) Tissue. *PloS One* 1, e0191631. doi: 10.1371/journal.pone.0191631

Campbell, K., Matero, I., Bellas, C., Turpin-Jelfs, T., Anhaus, P., Graeve, M., et al. (2022). Monitoring a Changing Arctic: Recent Advancements in the Study of Sea Ice Microbial Communities. *Ambio* 51 (2), 318–332. doi: 10.1007/s13280-021-01658-z

Cavalieri, D. J., and Parkinson, C. L. (2012). Arctic Sea Ice Variability and Trends 1979-2010. *Cryosphere.* 6, 881–889. doi: 10.5194/tc-6-881-2012

English, T. S. (1961). Some Biological Oceanographic Observations in the Central North Polar Sea Drift Station Alpha 1957-1958. *Arctic. Inst. North Am. Res. Paper.* 13, 1–80.

Fernández-Méndez, M., Wenzhöfer, F., Peeken, I., Sørensen, H. L., Glud, R. N., and Boetius, A. (2014). Composition, Buoyancy Regulation and Fate of Ice Algal Aggregates in the Central Arctic Ocean. *PloS One* 9, e107452. doi: 10.1371/journal.pone.0107452

Franks, J., and Stolz, J. F. (2009). Flat Laminated Microbial Mat Communities. *Earth Sci. Rev.* 96, 163–172. doi: 10.1016/j.earscirev.2008.10.004

Glud, R. N., Gundersen, J. K., and Ramsing, N. B. (2000). "Electrochemical and Optical Oxygen Microsensors for *in Situ* Measurements," in *In Situ Monitoring of Aquatic Systems—Chemical Analysis and Speciation.* Eds. J. Buffle and G. Horvai (Chichester: J Wiley & Sons).

Glud, R. N., Kühl, M., Kohls, O., and Ramsing, N. B. (1999). Heterogeneity of Oxygen Production and Consumption in a Photosynthetic Microbial Mat as Studies by Planar Optodes. *J. Phycol.* 35, 270–279. doi: 10.1046/j.1529-8817.1999.3520270.x

Glud, R. N., Kühl, M., Wenzhofer, F., and Rysgaard, S. (2002). Benthic Diatoms of a High Arctic Fjord (Young Sound, NE Greenland): Importance for Ecosystem Primary Production. *Mar. Ecol. Prog. Ser.* 238, 15–29. doi: 10.3354/meps238015

Glud, R. N., Ramsing, N. B., and Revsbech, N. P. (1992). Photosynthesis and Photosynthesis-Coupled Respiration in Natural Biofilms Quantified With Oxygen Microsensors. *J. Phycol.* 28 (1), 51–60. doi: 10.1111/j.0022-3646.1992.00051.x

Glud, R. N., Rysgaard, S., Turner, G., McGinnis, D. F., and Leakey, R. J. (2014). Biological- and Physical-Induced Oxygen Dynamics in Melting Sea Ice of the Fram Strait. *Limnol. Ocean.* 59, 1097–1111. doi: 10.4319/lo.2014.59.4.1097

Glud, R. N., Woelfel, J., Karsten, U., Kühl, M., and Rysgaard, S. (2009). Benthic Microalgal Production in the Arctic: Applied Methods and Status of the Current Database. *Bot. Marin.* 52, 559–571. doi: 10.1515/BOT.2009.074

Gosselin, M., Levasseur, M., Wheeler, P. A., Horner, R. A., and Booth, B. C. (1997). New Measurements of Phytoplankton and Ice Algal Production in the Arctic Ocean. *Deep. Sea. Res. Part II.* 44, 1623–1644. doi: 10.1016/S0967-0645(97)00054-4

K. Grasshoff, M. Erhardt and K. Kremling (Eds.) (1999). *Methods of Seawater Analysis* (London: Wiley), p. 632.

Hancke, K., and Glud, R. N. (2004). Temperature Effects on Respiration and Photosynthesis in Three Diatom-Dominated Benthic Communities. *Aquat. Micro. Biol.* 37, 265–281. doi: 10.3354/ame037265

Hancke, K., Hancke, T. B., Olsen, L. M., Johnsen, G., and Glud, R. (2008). Temperature Effects on Microalgal Photosynthesis-Light Responses Measured by O2 Production, Pulse-Amplitude-Modulated Fluorescence, and C-14 Assimilation. *J. Phycol.* 44 (2), 501–514. doi: 10.1111/j.1529-8817.2008.00487.x

Hancke, K., Lund-Hansen, L. C., Pedersen, S., King, M. d., Andersen, P., and Sorrell, B. K. (2018). Extreme Low Light Requirement for Algae Growth Underneath Sea Ice: A Case Study From Station Nord, NE Greenland. *J. Geophys. Res. Oceans.* 123, 985–1000. doi: 10.1002/2017JC013263

Hegseth, E. N. (1992). Sub-Ice Assemblages of the Barents Sea: Spice Composition, Chemical Composition, and Growth Rates. *Pol. Biol.* 12, 485–496. doi: 10.1007/BF00238187

Hodal, H., and Kristiansen, S. (2008). The Importance of Small-Celled Phytoplankton in Spring Blooms at the Marginal Ice Zone in the Northern Barents Sea. *Deep-Sea. Res. Part II: Topical Studies Oceanograp. - DEEP-SEA. Res. PT. II-TOP. ST. OCE.* 55, 2176–2185. doi: 10.1016/j.dsr2.2008.05.012

Jørgensen, B. B., and Revsbech, N. P. (1985). Diffusive Boundary Layers and the Oxygen Uptake of Sediments and Detritus. *Limnol. Ocean.* 30, 111–122. doi: 10.4319/lo.1985.30.1.0111

Jeffrey, S. W., Wright, S. W., and Zapata, M. (1999). Recent Advances in HPLC Pigment Analysis of Phytoplankton. *Mar. Freshw. Res.* 50, 879–896. doi: 10.1071/MF99109

Joy-Warren, H. L., van Dijken, G. L., Alderkamp, A. C., Leventer, A., Lewis, K. M., Selz, V., et al. (2019). Light is the Primary Driver of Early Season

Phytoplankton Production Along the Western Antarctic Peninsula. *J. Geophys. Res. Oceans* 124, 7375–7399. doi: 10.1029/2019JC015295

Katlein, C., Fernández-Méndez, M., Wenzhöfer, F., and Nicolaus, M. (2015). Distribution of Algal Aggregates Under Summer Sea Ice in the Central Arctic. *Pol. Biol.* 38, 719–731. doi: 10.1007/s00300-014-1634-3

Kivimae, C. (2007). *Carbon and Oxygen Fluxes in the Barents and Norwegian Seas: Production, Air-Sea Exchange and Budget Calculations. Doctoral Thesis* (University of Bergen, Bergen: Bergen Open Research Archive (uib.no)).

Kühl, M., Glud, R. N., Ploug, H., and Ramsing, N. B. (1996). Microenvironmental Control of Photosynthesis and Photosynthesis-Coupled Respiration in an Epilithic Cyanobacterial Biofilm. *J. Phycol.* 32, 799–812. doi: 10.1111/j.0022-3646.1996.00799.x

Lalande, C., Nöthig, E.-M., and Fortier, L. (2019). Algal Export in the Arctic Ocean in Times of Global Warming. *Geophys. Res. Lett.* 46, 5959–5967. doi: 10.1029/2019GL083167

Lee, S. H., Kim, B. K, J, H.-T., Park, J. W., Lee, J. H., Joo, H.-M., et al. (2015). Carbon Contribution of Sea Ice Floes in the Arctic Ocean. *Deep-Sea. Res. II.* 120, 35–42. doi: 10.1016/j.dsr2.2013.12.021

Lee, S. H., McRoy, P. C., Joo, H. M., Gradinger, R., Cui, X., Yun, M. S., et al. (2011). Holes in Progressively Thinning Arctic Sea Ice Lead to New Ice Algae Habitat. *Oceanography* 24 (3), 302–308. doi: 10.5670/oceanog.2011.81

Lee, S. H., Stockwell, D., Joo, H.-M., Son, Y. B., Kang, C.-K., and Whitledge, T. (2012). Phytoplankton Production From Melting Ponds on Arctic Sea Ice. *J. Geophys. Res. (Oceans)* 117, 4030. doi: 10.1029/2011JC007717

Lee, S., Stroeve, J., Tsamados, M., and Khan, A. L. (2020). Machine Learning Approaches to Retrieve Pan-Arctic Melt Ponds From Visible Satellite Imagery. *Remote Sens. Environ.* 247, 111919. doi: 10.1016/j.rse.2020.111919

Leu, E., Mundy, C. J., Assmy, P., Campbell, K., Gabrielsen, T. M., Gosselin, M., et al. (2015). Arctic Spring Awakening - Steering Principles Behind the Phenology of Vernal Ice Algal Blooms. *Prog. Oceanograp.* 139, 151–170. doi: 10.1016/j.pocean.2015.07.012

Li, Y. H., and Gregory, S. (1974). Diffusion of Ions in Sea-Water and in Deep-Sea Sediments. *Geochim. Et. Cosmochim. Acta* 38 (5), 703–714. doi: 10.1016/0016-7037(74)90145-8

Lund-Hansen, L. C., Hawes, I., Hancke, K., Salmansen, N., Nielsen, J. r. , Balslev, L., et al. (2020b). Effects of Increased Irradiance on Biomass, Photobiology, Nutritional Quality, and Pigment Composition of Arctic Sea Ice Algae. *Mar. Ecol. Prog. Ser.* 648, 95–110. doi: 10.3354/meps13411

Lund-Hansen, L. C., Hawes, I., Nielsen, M. H., Dahllöf, I., and Sorrell, B. (2018). Summer Meltwater and Spring Sea Ice Primary Production, Light Climate and Nutrients in an Arctic Estuary, Kangerlussuaq, West Greenland. *Arctic. Antarctic. Alpine. Res.* 50, e1414468-1-e1414468-11. doi: 10.1080/15230430.2017.1414468

Lund-Hansen, L. C., Markager, S., Hancke, K., Stratmann, T., Rysgaard, S., Ramløv, H., et al. (2015). Effects of Sea-Ice Light Attenuation and CDOM Absorption in the Water Below the Eurasian Sector of the Central Arctic Ocean. *Pol. Res.* 34, 23978. doi: 10.3402/polar.v34.23978

Lund-Hansen, L. C., Søgaard, D. H., Sorrell, B. K., Gradinger, R. , and Meiners, K. (2020a). *Arctic Sea Ice Ecology* (Cham, Switzerland: Springer Polar Series. Springer). 10.1007/978-3-030-37472-3.

Mackinney, G. (1941). Absorption of Light by Chlorophyll Solutions. *J. Biol. Chem.* 23, 315–322. doi: 10.1016/S0021-9258(18)51320-X

Meredith, M., Sommerkorn, M., Cassotta, S., Derksen, C., Ekaykin, A., Hollowed, A., et al. (2019). "Polar Regions," in *IPCC Special Report on the Ocean and Cryosphere in a Changing Climate*. Eds H.-O. Pörtner, D. C. Roberts, V. Masson-Delmotte, P. Zhai, M. Tignor, E. Poloczanska, K. Mintenbeck, A. Alegría, M. Nicolai, A. Okem, J. Petzold, B. Rama and N. M Weyer. (Geneva, Switzerland: Intergovernmental Panel on Climate Change).

Polashenski, C., Perovich, D., and Courville, Z. (2012). The Mechanisms of Sea Ice Melt Pond Formation and Evolution. *J. Geophys. Res.* 117 (C1), C01001. doi: 10.1029/2011JC007231

Quesada, A., Fernandez-Valiente, E., Hawes, I., and Howard-Williams, C. (2008). *Benthic Primary Production in Polar Lakes and Rivers. In: Polar Lakes and Rivers: Limnology of Arctic and Antarctic Aquatic Ecosystems*. Eds. W. F. Vincent and J. Layborn-Parry (Oxford, UK: Oxford Scholarship Online). doi: 10.1093/acprof:oso/9780199213887.001.0001

Revsbech, N. P. (1989). An Oxygen Microsensor With a Guard Cathode. *Limnol. Ocean.* 34, 474–478. doi: 10.4319/lo.1989.34.2.0474

Revsbech, N. P., and Jorgensen, B. B. (1983). Photosynthesis of Benthic Microflora Measured With High Spatial-Resolution by the Oxygen Microprofile Method - Capabilities and Limitations of the Method. *Limnol. Oceanogr.* 28 (4), 749–756. doi: 10.4319/lo.1983.28.4.0749

Rodriguez, F., Chauton, M., Johnsen, G., Andresen, K., Olsen, L. M., and Zapata, M. (2006). Photoacclimation in Phytoplankton: Implications for Biomass Estimates, Pigment Functionality and Chemotaxonomy. *Mar. Biol.* 148, 963–971. doi: 10.1007/s00227-005-0138-7

Sørensen, H. L., Thamdrup, B., Jeppesen, E., Rysgaard, S., and Glud, R. N. (2017). Nutrient Availability Limits Biological Production in Arctic Sea Ice Melt Ponds. *Pol. Biol.* 40, 1593–1606. doi: 10.1007/s00300-017-2082-7

Stemann-Nielsen, E. (1952). The Use of Radio-Active Carbon (C^{14}) for Measuring Organic Production in the Sea. *ICES. J. Mar. Sci.* 18, 117–140. doi: 10.1093/icesjms/18.2.117

Tamelander, T., Reigstad, M., Hop, H., and Ratkova, T. (2009). Ice Algal Assemblages and the Vertical Export of Organic Matter From Sea Ice in the Barents Sea and Nansen Basin (Arctic Ocean). *Pol. Biol.* 32, 1261–1273. doi: 10.1007/s00300-009-0622-5

Tomas, C. R. (1997). *Identifying Marine Phytoplankton* (San Diego: Academic Press Inc), p. 874.

Vincent, W. F., Downes, M. T., Castenholz, R. W., and Howard-Williams, C. (1993). Community Structure and Pigment Organisation of Cyanobacteria-Dominated Microbial Mats in Antarctica. *Europ. J. Phycol.* 28, 213–221. doi: 10.1080/09670269300650321

Wassmann, P., Carroll, J., and Bellerby, R. G. J. (2008). Carbon Flux and Ecosystem Feedback in the Northern Barents Sea in an Era of Climate Change: An Introduction. *Deep. Sea. Res. Part II.: Top. Stud. Oceano.* 55, 2143–2153. doi: 10.1016/j.dsr2.2008.05.025

Woelfel, J., Schumann, R., Peine, F., Flohr, A., Kruss, A., Tegowski, J., et al. (2010). Microphytobenthos of Arctic Kongsfjorden (Svalbard, Norway): Biomass and Potential Primary Production Along the Shoreline. *Pol. Biol.* 33, 1239–1253. doi: 10.1007/s00300-010-0813-0

Wunderling, N., Willeit, M., Donges, J. F., and Winkelmann, R. (2020). Global Warming Due to Loss of Large Ice Masses and Arctic Summer Sea Ice. *Nat. Commun.* 11, 5177. doi: 10.1038/s41467-020-18934-3

Zapata, M., Rodriguez, F., and Garrido, J. L. (2000). Separation of Chlorophylls and Carotenoids From Marine Phytoplankton: A New HPLC Method Using a Reversed Phase C-8 Column and Pyridine-Containing Mobile Phases. *Mar. Ecol. Prog. Ser.* 195, 29–45. doi: 10.3354/meps195029